A new method for measuring grain displacements in granular materials by X-ray computed tomography

M.H. Khalili, Sébastien Brisard, Michel Bornert, Jean-Michel Pereira, Matthieu Vandamme, Jean-Noël Roux

A new method for measuring grain displacements in granular materials by X-ray computed tomography

M-H. Khalili*, S. Brisard, M. Bornert, J-M. Pereira, M. Vandamme and J-N. Roux

Université Paris-Est, Laboratoire Navier (UMR 8205), CNRS, ENPC, IFSTTAR, F-77455 Marne-la-Vallée

*presenting author : mohamed-hassan.khalili@enpc.fr

We aim to measure the individual grain displacements in a granular material under constant load (creep). X-ray computed tomography imaging provides images of the granular medium microstructure during the experiment, and discrete volumetric image correlation (DV-DIC) [1] allows the determination of the grain individual rigid body motion from the reconstructed tomography images. However, for short-term creep, and time-resolved experiments in general, the sample evolutions can be very quick and occur before the full tomography scan is complete. This constitutes a serious limitation of standard experimental procedures for the investigation of the micromechanics of the creep of granular media at the grain scale.

We present a new method for measuring grain displacements, that overcomes the above-mentioned limitation. Indeed, in a granular material, assuming no breakage occurs, each grain undergoes a rigid body motion. Therefore, the displacement field reduces to a set of six degrees of freedom per grain. This suggests that the information contained in a full set of projections (necessary to perform an accurate 3D reconstruction) is excessively redundant for the determination of the grain displacements. Our method requires only few projections of the sample at its current state, thus reducing dramatically the acquisition time. Displacements are estimated from the projections directly, without 3D reconstruction.

Our method is formulated as an inverse problem. A forward model based on Beer-Lambert's law is developed to efficiently perform numerical projections. The grain displacements are estimated by fitting the numerical projections to experimental projections of the current state of the sample.

We also study the sensitivity of the estimated displacements to image noise, both numerically and through a theoretical model which highlights the influence of the setup parameters on the measurements.

The method has been validated and its accuracy assessed against 2D and 3D numerical experiments on virtual microstructures.

Keywords: Displacements measurement, X-ray tomography, granular medium

1 Introduction

Investigating micro-scale mechanisms in granular materials is an increasing trend to understand their macro-scale behavior. X-ray imaging tomography is an efficient way to characterize the evolution at the scale of the grain during a mechanical experiment. Once the tomographic projections are acquired and 3D image reconstruction is performed, Digital Image Correlation techniques (DIC) [2, 3, 4] can be used to measure strain fields. While this approach considers the medium as a continuum, more recent works provide a discrete analysis of the medium where grains are individuated, as for the Discrete Volumetric DIC (DV-DIC) [1] or ID-Track [5] techniques. In this work, we present an alternative approach, where displacements of grains are directly measured on the tomographic projections (as opposed to the reconstruction). This new approach allows us to reduce the number of required projections and thus the acquisition time, so that it is better suited to study time-resolved phenomena.

2 General principles

The proposed method consists in resolving an inverse problem that was formulated on the tomographic projections rather than the reconstructed images. From a reconstruction of the initial state, grains are individuated in order to compute numerical projections where a trial rigid body motion is applied to every grain. Then, we estimate the grain displacements in the current state by fitting the numerical projections to the measured experimental projections of the current state. This fitting is performed through minimization of an objective function that we define as follows:

$$\mathrm{F}(\mathbf{q}) = \sum_{\theta} \sum_{\underline{p}} \left(\hat{P}(\theta, \underline{p}; \mathbf{q}) - P(\theta, \underline{p}) \right)^2 \tag{1}$$

where $\mathbf{q}$ is a column-vector that gathers the parameters defining the rigid body motion of each grain. The forward model $\hat{P}(\theta, \underline{p}; \mathbf{q})$ gives a numerical projection of the medium for a trial generalized displacement $\mathbf{q}$; $\underline{p}$ is the pixel of the detector, and θ is the rotation angle of the sample stage. It is detailed in the next section, and more details can be found in [6]. $P(\theta, \underline{p})$ is the measured experimental projection.

3 Forward problem

The forward problem aims to compute numerical projections of the granular medium for any given trial generalized displacement $\mathbf{q}$. For a grain i in some reference position in the sample, the intensity measured at the pixel $\underline{p}$ of the detector is given by the Beer–Lambert's law as follows:

$$I(\underline{p}) = I_0 \exp\left(- \int \mu^{(i)} \left(\underline{p} + s \underline{T}(\underline{p}) \right) \mathrm{d}s \right), \tag{2}$$

where I_0 is the initial X-ray intensity, $\underline{T}(\underline{p})$ denotes the direction of the ray going from the source to the center of pixel $\underline{p}$, and crossing the grain. s denotes the arc-length along the

ray $(\underline{p}, \underline{T}(\underline{p}))$ and $\underline{x} \mapsto \mu^{(i)}(\underline{x})$ is a mapping of the local linear attenuation coefficient of grain i in some reference position. In what follows we define the projection as the integral of the attenuation. Assuming the sample stage to be rotated by an angle θ, let $\hat{P}^{(i)}(\theta, \underline{p}; \mathbf{q}^{(i)})$ denote the projection at pixel $\underline{p}$ of the i-th grain subjected to the rigid body motion defined by $\mathbf{q}^{(i)}$. Then, from Eq. (2)

$$\hat{P}^{(i)}(0, \underline{p}; \mathbf{0}) = \int \mu^{(i)}\left(\underline{p} + s\underline{T}(\underline{p})\right) \mathrm{d}s, \tag{3}$$

Given a segmented image of the medium, the projection of the medium can be evaluated as the sum of the projections of the individual grains moved according to their respective rigid body motion parameters. With the assumption of null absorption outside the grain,

$$\hat{P}(\theta, \underline{p}; \mathbf{q}) = \sum_i \hat{P}^{(i)}(\theta, \underline{p}; \mathbf{q}^{(i)}), \tag{4}$$

where $\mathbf{q}^{(i)}$ is the part of $\mathbf{q}$ containing the degrees of freedom of the i-th grain. $\mathbf{q}^{(i)}$ can also be expressed as a rotation tensor $\underline{\underline{\Omega}}^{(i)}$ and translation vector $\underline{u}^{(i)}$, by choosing an adequate parameterization [7]. Now, consider that the grain underwent a rigid body motion $(\underline{u}^{(i)}, \underline{\underline{\Omega}}^{(i)})$ with respect to its reference position and that the sample is rotated by an angle θ (the corresponding rotation tensor is $\underline{\underline{R}}_\theta$), then

$$\hat{P}^{(i)}(\theta, \underline{p}; \mathbf{q}^{(i)}) = \int \mu^{(i)}\left(\underline{\underline{\Omega}}^{(i)\,T} \cdot \left[\underline{\underline{R}}_\theta^T \cdot \left(\underline{p} + s\underline{T}(\underline{p})\right) - \underline{u}^{(i)}\right]\right) \mathrm{d}s. \tag{5}$$

In practice, the attenuation field is voxelized, which leads us to evaluate (5) for every voxel. It reduces to the summation of the intersection lengths of the ray with voxels it crosses weighted by the attenuation coefficient at that voxel. This summation is efficiently evaluated by means of Siddon's algorithm [8]. However, a further numerical gain can be made if we only consider the set of rays that actually intersect a given grain. This was achieved by the introduction of a minimal bounding box that contains the grain.
For the applications of the method, an improved version of Siddon's algorithm proposed by Jacobs [9] was implemented and adapted to our context.

4 Numerical test of the method

In this section, we present a numerical validation of the method. Results of simulations, based on numerically generated "experimental" projections, are given for planar 2D and full 3D situations.

Materials To perform numerical experiments, we need a segmented reference image of the medium. For the 2D case, we obtained this image from 30 grains taken from a cross section of a real tomography image of a Hostun sand. These grains were randomly distributed in an array of size 500x500 pixels to form an aggregate of 300 grains. For the 3D case, two grains extracted from the same sand image were distributed in a volume of 100x100x100 voxels.

Simulations For both cases, we create experimental projections by applying a displacement field to the grains, with translations of the grain centers randomly chosen between -1 and 1 pixel and rotation angles between -0.1 and 0.1 radians. These projections were computed by means of the forward model developed in Sec. 3. Then, we used a Levenberg–Marquart algorithm[1] to carry out the minimization starting from an initial guess $\mathbf{q}_0$ equal to the reference state.

Results In the 2D case, simulations of individual grains and of groups of grains (up to 300 grains) were successful with only two projections for individual grains and six projections for the group simulations.
For the 3D case, we ran simulations with two grains. Two different simulations are presented here, in parallel beam and cone beam projections. The results show that for the cone beam case, the simulation returns the exact applied displacements, while in the parallel case an error on the translation component along the sample rotation axis is observed. This is due to the fact that in parallel beam setup a translation along this direction, with an amplitude below the pixel size, does not induce any change to the simulated projections and hence, cannot be measured.
To deal with this issue improvements of the forward model taking into account a heterogeneous attenuation inside voxels and integration of rays over the width of the pixels will be explored.

5 Accuracy assessment

In this section, we evaluate the influence of noise in the projections on the accuracy of the methods. As expected, introducing noise in the previously presented simulations induces errors on the solution, i.e. a deviation of the minimum of the objective function with respect to its value without noise. This deviation can be characterized by its bias and its standard deviation from a statistical set of randomly chosen image noise. Following the procedures described in [10, 11], this error can also be evaluated by a theoretical perturbation analysis, assuming a white noise with uniform standard deviation σ. To do so, we assume the error on displacement sufficiently small so that the objective function can be linearized about its minimum without noise $\mathbf{q}^\star$, and write:

$$\mathbf{q} = \delta\mathbf{q} + \mathbf{q}^\star. \tag{6}$$

The objective function with noise $N(\theta, \underline{p})$ added to the experimental projections reads:

$$\mathrm{F}^N(\mathbf{q}) = \sum_{\theta,\underline{p}} \left[\hat{P}(\theta, \underline{p}; \mathbf{q}) - \left(\hat{P}(\theta, \underline{p}; \mathbf{q}^\star) + N(\theta, \underline{p})\right)\right]^2 \tag{7}$$

According to the noiseless simulations $P(\theta, \underline{p})$ was taken equal to $\hat{P}(\theta, \underline{p}; \mathbf{q}^\star)$. Then, assuming the perturbation induced by noise is sufficiently small, we can write:

$$\hat{P}(\theta, \underline{p}; \mathbf{q}) = \hat{P}(\theta, \underline{p}; \mathbf{q}^\star) + \delta\mathbf{q}^T \cdot \frac{\partial \hat{P}}{\partial \mathbf{q}}\left(\theta, \underline{p}; \mathbf{q}^\star\right), \tag{8}$$

[1] Provided by Scipy package for Python

and get the expression of the error:

$$\delta\mathbf{q} = \mathbf{M}^{-1} \cdot \mathbf{b}^N \tag{9}$$

with :

$$\mathbf{M} = \sum_{\theta,\underline{p}} \frac{\partial \hat{P}}{\partial \mathbf{q}}\left(\theta, \underline{p}; \mathbf{q}^\star\right) \cdot \frac{\partial \hat{P}}{\partial \mathbf{q}}^T \left(\theta, \underline{p}; \mathbf{q}^\star\right) \qquad \mathbf{b}^N = \sum_{\theta,\underline{p}} N(\theta, \underline{p}) \frac{\partial \hat{P}}{\partial \mathbf{q}}\left(\theta, \underline{p}; \mathbf{q}^\star\right) \tag{10}$$

Assuming uniform white noise over the pixels $(\theta, \underline{p})$, we obtain the statistical expectation $\mathrm{E}[\delta\mathbf{q}]$ and variance $\mathrm{var}(\delta\mathbf{q})$ of this error:

$$\mathrm{E}\left[\delta\mathbf{q}\right] = \mathbf{M}^{-1} \cdot \mathrm{E}[\mathbf{b}^N] = 0 \qquad \mathbf{\Sigma}^2 = \mathrm{var}\left(\delta\mathbf{q}\right) = \mathrm{E}[\delta\mathbf{q} \cdot \delta\mathbf{q}^T] = \sigma^2\mathbf{M}^{-1} \tag{11}$$

Further developments show that the matrix $\mathbf{M}$ is block diagonal with blocks associated to individual grains, which means that the error induced by white image noise on the results of one grain displacements does not depend on the other grains. This property allows us to study individual grain for the evaluations of matrix $\mathbf{M}$.

Figure 1 shows the evolution of the standard deviation $\sqrt{\Sigma^2_{11}}$ of a displacement of one grain in the 2D case. It corresponds to the horizontal translation along the plane of the detector. It was computed in two different ways. The first way is by numerical estimation of the matrix $\mathbf{M}$, where its components were computed by means of the forward model developed in 3. The second method is by running 10 simulations with different noise realizations and directly compute the standard deviation from the results (Monte-Carlo simulations). The signal to noise ratio $P_{\max}/\sigma$ was set to 500. This value gives a noise level that is slightly greater than the maximal noise level observed in our local tomography facility.

The two computations were performed for several numbers of projections. We can see that the results from the model are in good agreement with simulations. We also observe how increasing the number of projections reduces the noise error. Similar behaviors are observed for the other components of the translation and the rotation. At about 30 projections, the standard deviation amplitudes are comparable to theoretical ones estimated for a cubic shape in [10] for standard DV-DIC routines. At 60 projections the values of errors become lower by one order of magnitude and start to stabilize with respect to the increase of the number of projections.

6 Conclusion

In this work, we developed a new technique that bypasses the 3D reconstruction stage, and measures the displacements directly from tomographic projections. The acquisition time is dramatically reduced, which makes this technique well suited to investigate fast evolutions such as short-term creep. We presented in this paper a numerical validation to illustrate the feasibility of this technique. Finally, we probed the effect of image noise and proposed a model to estimate the error induced by noise.

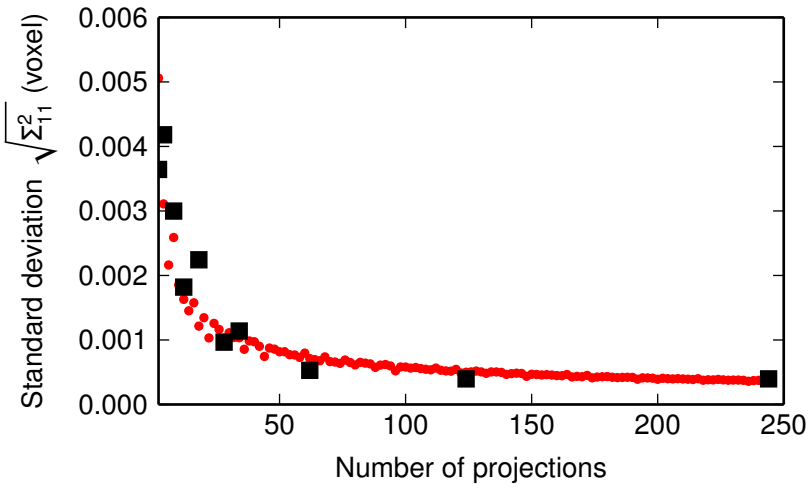

Figure 1 – Standard deviation of the estimated translation of the center of the grains, versus the number of used projections: Black squares indicate results of Monte-Carlo simulations (using 10 realizations for each simulation). The red points are the standard deviation estimated from our model [see Eqs. (9), (10) and (11)].

Acknowledgment: This work has benefited from a French government grant managed by ANR within the frame of the national program Investments for the Future ANR-11-LABX-022-01

References

[1] S-A. Hall, M. Bornert, J. Desrues, , Y. Pannier, N. Lenoir, , G. Viggiani, and P. Bésuelle. Discrete and continuum analysis of localised deformation in sand using X-ray μCT and volumetric digital image correlation. *Géotechnique*, 60(5):315–322, January 2010.

[2] B. K. Bay, T. S. Smith, D. P. Fyhrie, and M. Saad. Digital volume correlation: Three-dimensional strain mapping using X-ray tomography. *Experimental Mechanics*, 39(3):217–226, 1999.

[3] M. Bornert, J-M. Chaix, P. Doumalin, J-C. Dupré, T. Fournel, D. Jeulin, E. Maire, M. Moreaud, and H. Moulinec. Mesure tridimensionnelle de champs cinématiques par imagerie volumique pour l'analyse des matériaux et des structures. *Instrumentation, Mesure, Métrologie*, 4(3-4):43–88, 2004.

[4] N. Lenoir, M. Bornert, J. Desrues, P. Bésuelle, and G. Viggiani. Volumetric digital image correlation applied to x-ray microtomography images from triaxial compression tests on argillaceous rock. *Strain*, 43(3):193–205, 2007.

[5] E. Andò, S-A. Hall, G. Viggiani, J. Desrues, and P. Bésuelle. Grain-scale experimental investigation of localised deformation in sand: a discrete particle tracking approach. *Acta Geotechnica*, 7(1):1–13, November 2011.

[6] M-H. Khalili, S. Brisard, M. Bornert, J-M. Pereira, M. Vandamme, and J-N. Roux. Measuring grain displacements in a granular medium by means of X-ray microtomography: a reconstruction-free approach. In preparation.

[7] O. Rodrigues. Des lois géométriques qui régissent les déplacements d'un système solide dans l'espace, et de la variation des coordonnées provenant de ces déplacements considérés indépendamment des causes qui peuvent les produire. *Journal de Mathématiques Pures et Appliquées*, 5:380–440, 1840.

[8] R-L. Siddon. Fast calculation of the exact radiological path for a three-dimensional CT array. *Medical Physics*, 12(2):252, 1985.

[9] F. Jacobs and E. Sundermann. A fast algorithm to calculate the exact radiological path through a pixel or voxel space. *J. Comput. Inf. . . .*, 1998.

[10] Y. Pannier, N. Lenoir, and M. Bornert. Discrete volumetric digital image correlation for the investigation of granular type media at microscale: accuracy assessment. *EPJ Web of Conferences*, (Dic), 2010.

[11] S. Roux and F. Hild. Stress intensity factor measurements from digital image correlation: post-processing and integrated approaches. *International Journal of Fracture*, pages 1–37, 2006.